

Resonant nonlinearity management for nonlinear-Schrödinger solitons

Hidetsugu Sakaguchi¹ and Boris A. Malomed²

¹Department of Applied Science for Electronics and Materials,
Interdisciplinary Graduate School of Engineering Sciences,
Kyushu University, Kasuga, Fukuoka 816-8580, Japan

²Department of Interdisciplinary Studies,
School of Electrical Engineering, Faculty of Engineering,
Tel Aviv University, Tel Aviv 69978, Israel

November 18, 2018

Abstract

We consider effects of a periodic modulation of the nonlinearity coefficient on fundamental and higher-order solitons in the one-dimensional NLS equation, which is an issue of direct interest to Bose-Einstein condensates in the context of the Feshbach-resonance control, and fiber-optic telecommunications as concerns periodic compensation of the nonlinearity. We find from simulations, and explain by means of a straightforward analysis, that the response of a fundamental soliton to the weak perturbation is resonant, if the modulation frequency ω is close to the intrinsic frequency of the soliton. For higher-order n -solitons with $n = 2$ and 3, the response to an extremely weak perturbation is also resonant, if ω is close to the corresponding intrinsic frequency. More importantly, a slightly stronger drive splits the 2- or 3-soliton, respectively, into a set of two or three moving fundamental solitons. The dependence of the threshold perturbation amplitude, necessary for the splitting, on ω has a resonant character too. Amplitudes and velocities of the emerging fundamental solitons are accurately predicted, using exact and approximate conservation laws of the perturbed NLS equation.

PACS numbers: 03.75.Lm, 05.45.Yv, 42.65.Tg

1 Introduction

The nonlinear Schrödinger (NLS) equation is a universal model of weakly nonlinear dispersive media [1, 2]. The existence and stability of solitons in the one-dimensional (1D) version of the NLS equation with constant coefficients is a well-established fact, which has important implications in various areas of physics.

In particular, solitons in fiber-optic telecommunications [3] and quasi-1D Bose-Einstein condensates (BECs) with attractive interactions between atoms [4], have drawn a great deal of interest.

A new class of dynamical problems, which also have a vast potential for physical applications, emerges in the investigation of soliton dynamics in extended versions of the NLS equation, in which coefficients are periodic functions of the evolutional variable. A well-known example is a nonlinear fiber-optic link subjected to *dispersion management* (DM), which implies that the dispersion coefficient periodically alternates between positive and negative values. The DM links support a family of stable temporal solitons (see, e.g., Refs. [5], and also Ref. [6]). Somewhat similar is a *waveguide-antiwaveguide* system, which can be realized in the spatial domain (planar optical waveguides). In the latter case, a light beam is transmitted through a periodic concatenation of nonlinear waveguiding and antiwaveguiding segments [7]. A common feature of the latter system with the DM is that the coefficient which periodically jumps between positive and negative values also belongs to the linear part of the equation.

Another technique that may be useful for optical telecommunications is *nonlinearity management* (NLM), which assumes that the coefficient in front of the nonlinear term periodically changes its sign. An advantage offered by the NLM is a possibility to compensate the nonlinear phase shift accumulating in pulses due to the Kerr nonlinearity of the optical fiber [8]. In practical terms, the NLM can be implemented by dint of elements with a strong quadratic ($\chi^{(2)}$) nonlinearity, which are periodically inserted into the fiber link. The $\chi^{(2)}$ elements can emulate a negative Kerr effect through the cascading mechanism [9]. Various other schemes of NLM in fiber-optic links were considered, including its combination with the DM, amplifiers, etc. [10]. A related scheme makes use of the NLM in soliton-generating lasers based on fiber rings [11]. The NLM for spatial solitons, which assumes alternation of self-focusing and self-defocusing nonlinear layers in planar [12] or bulk [13] waveguides, was introduced too.

All these systems may be regarded as examples of periodically inhomogeneous optical waveguiding media. Other examples belonging to the same general class are *tandem waveguides* (see Ref. [14] and references therein) and the *split-step model* [15]. These are built as a juxtaposition of linear segments alternating with ones featuring, respectively, quadratic or cubic nonlinearity. A common feature of the models of all these types is that they support *robust* solitons, despite a “naive” expectation that solitons would quickly decay, periodically hitting interfaces between strongly different elements of which the system is composed.

The above-mentioned optical media are described by the NLS equation, in which the role of the evolutional variable belongs to the propagation distance, while the remaining free variable is either the local time (for temporal solitons), or the transverse coordinate(s), in the spatial-domain models. Mathematically similar, but physically altogether different, models describe BECs in the 1D geometry. In that case, the corresponding NLS equation is usually called the Gross-Pitaevskii (GP) equation. It governs the evolution of the mean-field wave function ϕ in time (t), the other variable, x , being the coordinate along the

quasi-1D trap. In the normalized form, the GP equation is

$$i\phi_t = -\frac{1}{2}\phi_{xx} + U(x)\phi + g|\phi|^2\phi, \quad (1)$$

where $U(x)$ is the potential which confines the condensate, and the nonlinearity coefficient g is proportional to the scattering length of collisions between atoms. Two natural possibilities to introduce a time-periodic (ac) “management” in the BEC context are either through a periodic modulation of the confining potential, most typically in the form of $U(x, t) = \frac{1}{2}[\kappa_0 + \kappa_1 \cos(\omega t)]x^2$, or by means of time modulation of the scattering length, using the Feshbach resonance (FR) [16]. In the latter case, the nonlinearity coefficient in Eq. (1) takes the form of $g(t) = g_0 + g_1 \sin(\omega t)$. In either case, the modulation is generated by a combination of dc and ac magnetic fields applied to the BEC.

The GP equation with the periodically modulated strength of the trapping potential was considered for both $g > 0$ (when solitons do not exist, and the BEC as a whole is subjected to the “management”, including the 2D and 3D cases) [17], and $g < 0$, when the soliton is the basic dynamical object [18]. In particular, a parametric resonance is possible in the former case, and creation of an effectively trapping potential, while the underlying one is anti-trapping, having $\kappa_0 < 0$, by the high-frequency ac part of the potential (with large ω) was predicted in the latter case.

The periodic modulation of the nonlinearity coefficient through the “ac FR management” is an especially interesting possibility, as the FR is a highly efficient experimental tool, broadly used for the study of various dynamical properties of the BECs [16]. In particular, it has been predicted that the modulation through the ac FR makes it possible to preclude collapse and generate stable soliton-like structures in 2D (but not 3D) condensates [19]; in fact, this prediction is similar to the earlier considered possibility of the stabilization of 2D spatial optical solitons in a bulk waveguide subjected to the periodic NLM [13]. In the 1D model of the GP type, subjected to the NLM, various stable dynamical states, including Gaussian-shaped soliton-like objects, and ones of the Thomas-Fermi type, were studied in detail [20]. In addition, analysis based on averaged equations was developed, for this case, in Ref. [21] (similarly to the analysis elaborated in Ref. [18] for the case of the periodic modulation of the trapping potential).

The objective of this work is to study *resonance effects* produced by the ac FR management, i.e., harmonic modulation of the nonlinearity coefficient, in the dynamics of fundamental and higher-order 1D solitons in the NLS equation. We will focus on the case when the ac part of the nonlinear coefficient is small in comparison with its constant (dc) part g_0 , which accounts for the self-attraction in the BEC, and is normalized to be $g_0 = -1$. We also assume that the soliton’s width is much smaller than the effective size of the trap, hence the external potential may be dropped. The consideration of the GP equation without the trapping potential makes it possible to identify fundamental dynamical effects for the solitons induced by the ac FR management. In this connection, it is necessary to mention that, in the 1D case, the trapping potential is not a crucial

factor, on the contrary to the 2D and 3D cases, where the external potential plays a much more important role, in view of the intrinsic instability of the multi-dimensional NLS solitons.

Thus, we will be dealing with the normalized NLS equation in the form [cf. Eq. (1)]

$$i\phi_t + \frac{1}{2}\phi_{xx} + [1 + b \sin(\omega t)] |\phi|^2 \phi = 0, \quad (2)$$

where the amplitude b of the ac drive is small. Note that Eq. (2) conserves exactly two dynamical invariants: the norm, which is proportional to the number of atoms in the BEC,

$$N = \int_{-\infty}^{+\infty} |\phi(x)|^2 dx, \quad (3)$$

and the momentum,

$$P = i \int_{-\infty}^{+\infty} (\phi \phi_x^* - \phi^* \phi_x) dx. \quad (4)$$

We will demonstrate that the weak ac perturbation in Eq. (2) can generate strong effects, if the driving frequency ω is close to specific resonant values. These effects include intrinsic vibrations of the fundamental soliton and splitting of the higher-order ones. We will also propose analytical explanations to these effects. To the best of our knowledge, these results have not been reported before for the present simple model.

The rest of the paper is organized in the following way. The resonant effect of the periodic NLM on the fundamental soliton is reported in Section 2, and the resonant splitting of n -solitons with $n = 2$ and 3 is investigated in Section 3. Section 4 concludes the paper.

2 Resonant response of the fundamental soliton

2.1 Numerical results

First, we consider the action of the ac perturbation in Eq. (2) on the fundamental soliton, which, in the case $b = 0$, is

$$\phi_{\text{sol}}(x, t) = A \operatorname{sech}(A(x - x_0)) \exp(iA^2 t/2), \quad (5)$$

where A is an arbitrary amplitude. Numerical simulations of Eq. (2) were performed in a sufficiently large domain, $0 < x < L$, the initial condition corresponding to the soliton (5) placed at the center of the domain, $x_0 = L/2$. We have performed numerical simulations using the split-step Fourier method with 1024 Fourier modes. The system size is $L = 50$, and the time step for the numerical simulation is $\Delta t = 0.001$.

Figure 1(a) displays a typical example of the time evolution of the soliton's amplitude $|\phi(x = L/2)|$, under the action of the ac perturbation with a very small amplitude, $b = 0.0001$. The frequency of the beatings observed in this figure can be clearly identified as $\omega - \omega_{\text{sol}}$, where $\omega_{\text{sol}} \equiv A^2/2$ is the intrinsic

frequency of the unperturbed soliton (5). We have checked that the the beating frequency is independent of the system's size and the other details of the numerical scheme.

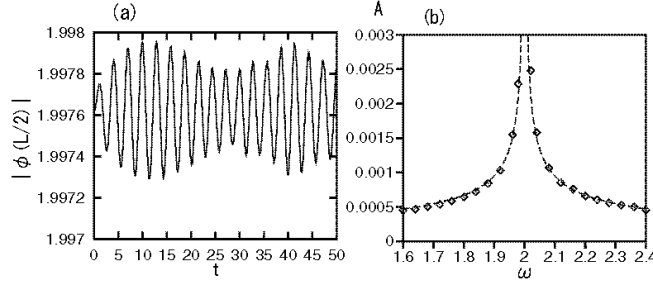


Figure 1: (a) A typical example of beatings in the evolution of the fundamental-soliton's amplitude under the action of a very weak perturbation in Eq. (2), with $b = 10^{-4}$ and $\omega = 2.2$. The amplitude of the initial unperturbed soliton is $A = 2$ (the corresponding soliton's frequency is $\omega_{\text{sol}} \equiv A^2/2 = 2$). (b) The difference between the maximum and minimum values of the soliton's amplitude vs. the perturbation frequency. The dashed line is a fitting curve, $0.0003 \cdot |\omega - 2|^{-1/2}$.

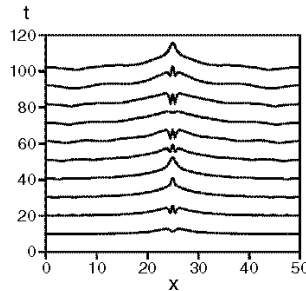


Figure 2: Direct numerical solution of the linearized equation (6) for the perturbation around the fundamental soliton, in the near-resonance case, with $\omega = 1.98$.

The main resonant effect for the fundamental soliton is displayed in Fig. 1(b), in the form of the difference between the maximum and minimum (in time) values of its amplitude versus the driving frequency ω . The resonance at $\omega = \omega_{\text{sol}} = 2$ (for $A = 2$) is obvious. The simulations do not reveal any noticeable subharmonic or higher-order resonance at frequencies $\omega = 1, 3$ or 4 . Due to the scaling invariance of Eq. (2), the plot shown in Fig. 1(b) does not pertain solely to the particular value of the soliton's amplitude, $A = 2$, but is actually a universal one. It is easy to verify that the ranges of the variables t

and x , which are shown in this and other figures, correspond, in the normalized units, to experimentally realistic configurations of the BECs in the quasi-1D geometry.

2.2 Perturbative analysis

In order to explain the resonance shown above, we look for a perturbed fundamental solution as $\phi(x, t) = \phi_{\text{sol}}(x, t) + \phi_{\text{pert}}(x, t)$, where the first term is the solution (5). Thus, we arrive at the driven linearized equation for the perturbation,

$$\begin{aligned} i(\phi_{\text{pert}})_t + \frac{1}{2}(\phi_{\text{pert}})_{xx} + A^2 \operatorname{sech}^2(Ax) \left(2\phi_{\text{pert}} + e^{iA^2 t} \phi_{\text{pert}}^* \right) \\ = \frac{i}{2} b A^3 \operatorname{sech}^3(Ax) \left[e^{i((A^2/2)+\omega)t} - e^{i((A^2/2)-\omega)t} \right]. \end{aligned} \quad (6)$$

The source of the resonant response is in the fact that the second term on the right-hand side of Eq. (6) becomes time-independent exactly at the resonance point, $\omega = \omega_{\text{sol}} \equiv A^2/2$. Figure 2 displays the evolution of the perturbation close to the resonance at $\omega = 1.98$, as found from direct numerical integration of the linearized equation (6), with the initial condition $\phi_{\text{pert}}(x) = 0$. As can be seen from the figure, the perturbation grows in time at the center, and simultaneously expands in space. Strictly speaking, the latter feature remains valid as long as the size of the region occupied by the expanding wave fields remains essentially smaller than the limit imposed by the confining field.

The linearized equation (6) is too difficult for an exact analytical solution. However, the observation that the characteristic spatial scale of the solution observed in Fig. 2 becomes much larger than the internal scale of the function $\operatorname{sech}(Ax)$ suggests that principal features of the solution can be understood from a simpler equation, in which the term $\sim \operatorname{sech}^2(Ax)$ on the left-hand side of Eq. (6) is neglected, and the source corresponding to the second term on the right-hand side is approximated by a δ -function:

$$i(\tilde{\phi}_{\text{pert}})_t + \frac{1}{2}(\tilde{\phi}_{\text{pert}})_{xx} = \text{const} \cdot \delta(x) e^{-i\Delta\omega \cdot t}, \quad \text{const} = \frac{i\pi}{4} b A^2, \quad (7)$$

where $\Delta\omega \equiv \omega - \omega_{\text{sol}}$, and $\text{const} \equiv (ib/2) A^3 \int_{-\infty}^{+\infty} \operatorname{sech}^3(Ax) dx$. Equation (7) can be solved by means of the Fourier transform. After straightforward manipulations, this yields

$$\tilde{\phi}_{\text{pert}}(x, t) = -\frac{\text{const}}{2\sqrt{\pi}} (1+i) e^{-i\Delta\omega \cdot t} \int_0^t \frac{dt'}{\sqrt{t'}} \exp\left(\frac{ix^2}{2t'} + i\Delta\omega \cdot t'\right). \quad (8)$$

Further consideration shows that, for $\Delta\omega < 0$, the asymptotic form of the solution (8) at $t \rightarrow \infty$ amounts to an exponentially localized stationary expression, which, by itself, is an exact solution to Eq. (7):

$$\tilde{\phi}_{\text{pert}}(x, t) = \frac{\text{const}}{\sqrt{2|\Delta\omega|}} \exp\left(i|\Delta\omega|t - \sqrt{2|\Delta\omega|}|x|\right). \quad (9)$$

In the case of $\Delta\omega > 0$, the asymptotic form of the general solution (8) corresponds to a symmetric region occupied by plane waves emitted by the central source at wavenumbers $k = \pm\sqrt{2\Delta\omega}$. The region expands in time with the group velocities $v_{\text{gr}} = k = \pm\sqrt{2\Delta\omega}$, so that the asymptotic form of the solution is

$$\tilde{\phi}_{\text{pert}}(x, t) \approx -i \frac{\text{const}}{\sqrt{2\Delta\omega}} \cdot \begin{cases} \exp\left(-i\Delta\omega \cdot t + i\sqrt{2\Delta\omega}|x|\right), & \text{if } |x| < \sqrt{2\Delta\omega}t, \\ 0, & \text{if } |x| > \sqrt{2\Delta\omega}t. \end{cases} \quad (10)$$

This asymptotic solution implies that the norm (3) of the expanding radiation field grows in time at the rate $dN_{\text{pert}}/dt = \sqrt{2/\Delta\omega}|\text{const}|^2$, which, in fact, is the rate at which the norm flows from the soliton to the radiation waves emitted under the action of the ac perturbation.

Both analytical expressions (9) and (10) feature the $|\Delta\omega|^{-1/2}$ factor, that perfectly fits the numerical data summarized in Fig. 1(b). Although these results, obtained for the weak time-periodic FR management, seem very simple, they have not been reported before, to the best of our knowledge. We also notice that the usual variational approximation (VA) for the NLS solitons, which is efficient in explaining a number of other perturbative effects [22], cannot account for the occurrence of the resonance at $\omega = \omega_{\text{sol}}$, because the VA neglects radiation effects, while the above consideration showed that it is exactly the radiation field which is amenable for the manifestations of the resonance.

The above results were obtained in the linear approximation, i.e., for a very small amplitude b of the ac drive in Eq. (2). At larger b , the perturbed soliton can either survive or decay into radiation. In fact, a stability region for the solitons in a similar model with a nonsmall perturbation, which differs from that in Eq. (2) by the form of the periodic modulation function, which is a piecewise-constant one, rather than harmonic, was drawn in Ref. [12] in the context of a model for spatial optical solitons in a layered waveguide. In the cases when a stable soliton established itself in the strongly perturbed (“strongly nonlinearly-managed”) system, its formation from the initial configuration (5) went through emission of radiation and, sometimes, separation of a small secondary pulse, while no pronounced resonance at $\omega = \omega_{\text{sol}}$ was observed. As we do not expect that the replacement of the piecewise-constant modulation function by the harmonic one should dramatically alter the stability region, we do not consider this issue here in detail.

3 Resonant splitting of higher-order solitons

3.1 Response to a very weak ac drive

As is well known, the unperturbed NLS equation gives rise to exact soliton solutions of order n , in the form of periodically oscillating breathers, which start from the initial conditions

$$\phi_0(x) = nA \operatorname{sech}(A(x - L/2)) \quad (11)$$

with an integer $n > 1$ [23] [the expression (11) assumes that the initial configuration is placed at the center of the integration domain]. The frequency of the shape oscillations (breathings) of the higher-order soliton is

$$\omega_{\text{br}} = 4A^2, \quad (12)$$

irrespective of the value of n .

Generally speaking, the higher-order solitons are unstable bound complexes of fundamental solitons, as, in the absence of perturbations, their binding energy is exactly zero, which is a known consequence of the exact integrability of the unperturbed NLS equation. Nevertheless, not any perturbation readily splits the higher-order soliton into its fundamental constituents; usually, the splitting is easily induced by specific nonconservative terms added to the NLS equation, such as the one accounting for the intra-pulse stimulated Raman scattering in optical fibers [3]. The consideration of dynamics of the higher-order solitons is also relevant, especially in the context of BECs, as the corresponding initial configurations can be created in the real experiment.

We have studied in detail the n -solitons up to $n = 5$. First, we consider the case of a very small driving amplitude, $b = 0.00005$. Figure 3 (a) displays oscillations of the amplitude $|\phi(x = L/2)|$ of the 2-soliton, which corresponds to the initial condition (11) with $n = 2$. The frequency of the basic oscillations coincides with ω_{br} , as given by the expression (12), while the frequency of the zoomed beatings in Fig. 3(b) can be clearly identified with $\omega - \omega_{\text{br}}$. The resonant character of the response of the 2-soliton to the weak NLM is obvious from Fig. 3(c).

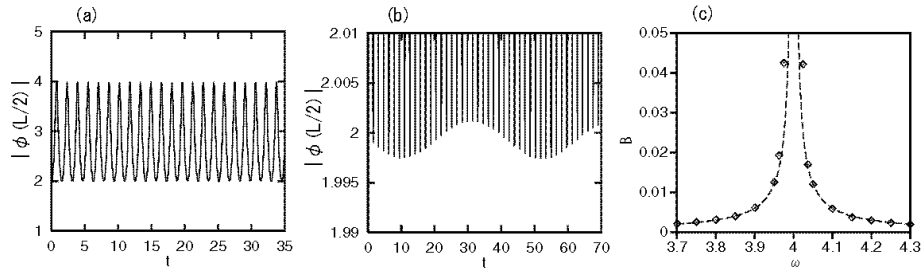


Figure 3: (a) Oscillations of the amplitude, $|\phi(x = L/2)|$, of the 2-soliton created by the initial condition (11) with $A = 1$, in the case of $b = 0.5 \times 10^{-4}$ and $\omega = 4.15$. (b) Zoom of the previous panel around minimum values of the amplitude, which reveals beatings at the frequency $\omega - \omega_{\text{br}}$. (c) The difference between the maximum and minimum values of the soliton's amplitude vs. the driving frequency ω . The dashed line is a fitting curve, $0.0006/|\omega - 4|$; note the difference of the fitting power, -1 , from that, $-1/2$, in Fig. 1(b).

Note that the exact solution for the n -soliton features not only the shape-oscillation frequency (12), but also an overall frequency of the phase oscillations,

which coincides with the above-mentioned frequency $\omega_{\text{sol}} = A^2/2$ for the fundamental soliton, provided that the initial condition is taken as in Eq. (11). In the simulations, we also observed a resonant response at $\omega = \omega_{\text{sol}}$, but this resonance was essentially weaker than the one at $\omega = \omega_{\text{br}}$. In particular, this is manifest in the fact that, as well as in the case of the fundamental soliton, the fit to the response around the former resonance is provided by the expression $|\omega - \omega_{\text{sol}}|^{-1/2}$, cf. Fig. 1(b), while the fit to the resonance at $\omega = \omega_{\text{sol}}$ demonstrates a more singular dependence, $\sim |\omega - \omega_{\text{br}}|^{-1}$, as seen in Fig. 3(c). Another qualitative difference between the two resonances is that the one at $\omega = \omega_{\text{br}}$, with a larger (but still small) forcing parameter b , leads to splitting of the higher-order solitons into fundamental ones, as shown below, while, in the case of the resonance at $\omega = \omega_{\text{sol}}$, the increase of b does not lead to the splitting.

3.2 Splitting of 2- and 3-solitons

Unlike the case of the fundamental soliton, the reaction of the higher-order ones to larger values of the forcing parameter was not studied before, therefore we have done it here. First, we aim to demonstrate that the 2-soliton readily splits into two moving fundamental pulses, if the driving frequency is close to the resonant value (12). The shape of each moving soliton is very close to that given by the commonly known exact solution, which can be obtained by application of the Galilean boost, with a velocity v , to the zero-velocity fundamental soliton (5),

$$\phi_{\text{sol}}(x, t) = A \operatorname{sech}(A(x - vt)) \exp [ivx + (i/2)(A^2 - v^2)t]. \quad (13)$$

Figure 4 displays the evolution of the wave function for the initial condition (11) with $n = 2$ in the resonant case ($A = 1$ and $\omega = 4$), with the driving amplitude $b = 0.0005$. The latter value is still very small, but larger by a factor of 10 than in the case shown in Fig. 3. The amplitudes of the two fundamental solitons, observed as a result of the splitting, are close to $A_1 = 3$ and $A_2 = 1$ [note that they exactly corresponds to the fundamental-soliton constituents of the original 2-soliton with $A = 1$, in terms of the inverse scattering transform (IST) [23]]. Velocities of the splinters were measured to be $v_1 = 0.00197$ and $v_2 = 0.0066$, respectively (with the ratio $v_1 : v_3 \approx 1 : 3$). At the end of the simulation run ($t = 1000$), the secondary solitons are found at the distance, respectively, 4.5 and 13.2 from the central point, $x = L/2$.

Similar near-resonant splittings were observed for n -solitons with $n > 2$. In particular, Fig. 5 shows this outcome for $n = 3$, which corresponds to the initial configuration (11) with $n = 3$, $A = 0.5$, $\omega = 1$ and $b = 0.0005$. This time, the splitting gives rise to three moving fundamental solitons, whose amplitudes are close to $A_1 = 2.5$, $A_2 = 1.5$, and $A_3 = 0.5$. As well as in the case of $n = 2$, these values correspond to the constituents of the original 3-soliton (with $A = 0.5$), in terms of the IST [23]. The velocities of the three splinters are $v_1 = -0.00146$, $v_2 = 0.0732$, and $v_3 = -0.0148$, so that the ratios between them are $v_1/v_2 \approx -1/5$ and $v_3/v_2 \approx -2$.

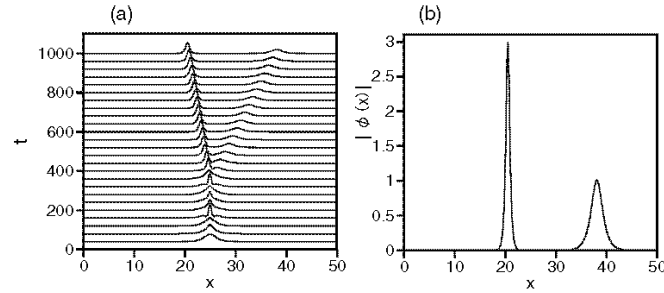


Figure 4: A typical example of the splitting of a 2-soliton [generated by the initial condition (11) with $n = 2$ and $A = 1$] into an asymmetric pair of moving fundamental solitons, under the action of the weak resonant drive, with $\omega = 4$ and $b = 0.0005$. (a) The evolution of $|u(x,t)|$. (b) The final configuration at $t = 1000$.

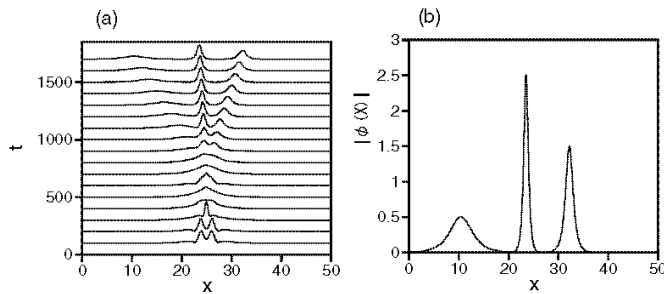


Figure 5: The same as in Fig. 4 for the 3-soliton, generated by the initial configuration (11) with $n = 3$ and $A = 0.5$. In this case, the forcing frequency and amplitude are $\omega = 1$ and $b = 0.0005$.

These results can be summarized in the form of diagrams which show the minimum (threshold) value of the forcing amplitude b , necessary for the splitting, versus the driving frequency ω . The splitting of the 2- and 3-solitons was registered if it took place in the simulations of Eq. (2) that were run up to the time, respectively, $t = 600$ or $t = 2000$ (still longer simulations did not give rise to any essential difference in the results). As is seen from Fig. 6, for both 2- and 3-solitons these dependences clearly have a resonant shape, with sharp minima at the frequency given by Eq. (12). It is not quite clear why the forcing amplitude required for the splitting is very small but finite even exactly at the resonance point. This may be related to the accuracy of the numerical scheme and/or the finite size of the integration domain. Similar observations were also made in simulations of the n -solitons with $n = 4$ and 5.

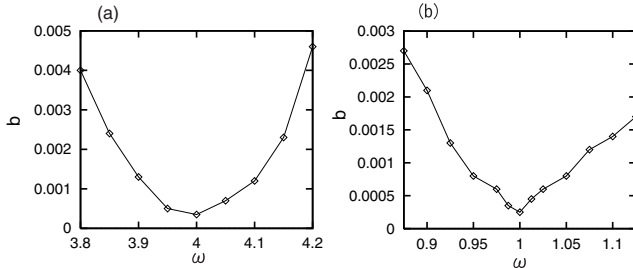


Figure 6: The minimum values of the amplitude of the ac perturbation, necessary for the splitting of the 2-soliton (a) and 3-soliton (b), as functions of the driving frequency. The initial condition is taken in the form of Eq. (11) with, respectively, $n = 2$ and $A = 1$, or $n = 3$ and $A = 0.5$. In both cases, the sharp minimum exactly corresponds to the resonant frequency, as predicted by Eq. (12).

3.3 Analytical results

The amplitudes and velocities of the fundamental solitons, into which the higher-order ones split, can be predicted in an analytical from. As it was already mentioned above, the amplitudes of the secondary solitons coincide with those which correspond to the constituents (eigenvalues) of the corresponding original n -soliton in terms of the IST. However, the velocities of the emerging fundamental solitons cannot be forecast this way, as, in terms of the IST, they are zero when the fundamental solitons are bound into a higher-order one.

Nevertheless, both the amplitudes and velocities of the final set of the solitons can be predicted in a different way, using the exact and nearly exact conservation laws of Eq. (2). Indeed, there are two exact dynamical invariants, (3) and (4), and, in addition to that, the unperturbed NLS equation has an infinite series of

higher-order dynamical invariants, starting from the Hamiltonian,

$$H = \frac{1}{2} \int_{-\infty}^{+\infty} (|\phi_x|^2 - |\phi|^4) dx. \quad (14)$$

Two next invariants, which do not have a straightforward physical interpretation, are [2]

$$I_4 = \frac{1}{2} \int_{-\infty}^{+\infty} (\phi \phi_{xxx}^* + 3\phi \phi_x^* |\phi|^2) dx,$$

$$I_5 = \frac{1}{4} \int_{-\infty}^{+\infty} \left[|\phi_{xx}|^2 + 2|\phi|^6 - ((|\phi|^2)_x)^2 - 6|\phi_x|^2 |\phi|^2 \right] dx. \quad (15)$$

In the case of the splitting of the 2-soliton (11) with the amplitude A , the exact conservation of the norm (3) and approximate conservation of the Hamiltonian (14) yield the following relations between A and the amplitudes $A_{1,2}$ of the emerging fundamental solitons (splinters): $4A = A_1 + A_2$, and $28A^3 \approx A_1^3 + A_2^3$ (the latter relation neglects small kinetic energy of the emerging solitons). These two relations immediately yield $A_1 = 3A$ and $A_2 = A$, which coincides with the the above-mentioned numerical results, as well as with the predictions based on the set of the 2-soliton's IST eigenvalues. Furthermore, the exact momentum conservation yields a relation involving the velocities $v_{1,2}$ of the secondary solitons, $A_1 v_1 + A_2 v_2 = 0$. With regard to the ratio $A_1/A_2 = 3$, this implies $v_1/v_2 = -A_2/A_1 = -1/3$. This relation is indeed consistent with the aforementioned numerical results, although the absolute values of the velocities cannot be predicted this way.

Similarly, in the case of the splitting of the 3-soliton, the exact conservation of N and approximate conservation of H and I_5 [see Eq. (15)] yield the relations (which again neglect small kinetic terms, in view of the smallness of the observed velocities) $9A = A_1 + A_2 + A_3$, $153A^3 \approx A_1^3 + A_2^3 + A_3^3$, and $3369A^5 \approx A_1^5 + A_2^5 + A_3^5$. A solution to this system of algebraic equations is $A_1 = 5A$, $A_2 = 3A$, $A_3 = A$, which are the same values that were found from the direct simulations, and can be predicted as the IST eigenvalues. The conservation of P and I_4 gives rise to further relations, $A_1 v_1 + A_2 v_2 + A_3 v_3 = 0$ and $(A_1 v_1^3 - A_1^3 v_1) + (A_2 v_2^3 - A_2^3 v_2) + (A_3 v_3^3 - A_3^3 v_3) = 0$. If the velocities $v_{1,2}$ are small, it follows from here that $v_1/v_2 = -(A_2^3 - A_2 A_3^2)/(A_1^3 - A_1 A_3^2) = -1/5$, and $v_3/v_2 = -(A_2^3 - A_2 A_1^2)/(A_3^3 - A_3 A_1^2) = -2$. These results for the velocities are consistent with the numerical situation observed in Fig. 5.

4 Conclusion

In this work, we have addressed a simple model, based on the NLS equation, which describes an attractive Bose-Einstein condensate (BEC) in a quasi-1D trap, with the nonlinearity strength subjected to a weak time-periodic (ac) modulation (that can be imposed by means of the Feshbach-resonance technique). The same model describes the nonlinearity management in periodically inhomogeneous optical waveguides.

It was found from direct simulations, and explained by means of a straightforward perturbative expansion, that the response of a fundamental soliton, in the form of temporal beatings of its amplitude, to the weak ac perturbation is resonant when the driving frequency ω is close to the soliton's intrinsic frequency. For n -solitons (breathers), with $n = 2$ and 3 , the response to an extremely weak drive is also resonant, if ω is close to the breathing frequency. More interestingly, a slightly stronger drive gives rise to splitting of the 2- and 3-solitons into sets of two or three moving fundamental solitons, respectively. The dependence of the minimum perturbation amplitude, which is necessary for the splitting, on ω has a clearly resonant character too. The amplitudes of the splinter solitons, and the ratio of their velocities, can be easily predicted on the basis of the exact and approximate conservation laws of the perturbed NLS equation.

Acknowledgment

The work of B.A.M. was partially supported by the grant No. 8006/03 from the Israel Science Foundation.

References

- [1] G. B. Whitham. *Linear and Nonlinear Waves* (John Wiley & Sons: New York, 1974).
- [2] V. E. Zakharov, S. V. Manakov, S. P. Novikov, and L. P. Pitaevskii. *Theory of Solitons* (Consultants Bureau: New York, 1984)
- [3] A. Hasegawa and Y. Kodama. *Solitons in Optical Communications* (Oxford University Press: New York, 2004).
- [4] K. E. Strecker, G. B. Partridge, A. G. Truscott, and R. G. Hulet, *Nature* **417**, 150 (2002); L. Khaykovich, F. Schreck, G. Ferrari, T. Bourdel, J. Cubizolles, L. D. Carr, Y. Castin, and C. Salomon, *Science* **296**, 1290 (2002); L. D. Carr and J. Brand, *Phys. Rev. Lett.* **92**, 040401 (2004).
- [5] A. Berntson, N.J. Doran, W. Forysiak, and J. H. B. Nijhof, *Opt. Lett.* **23**, 900 (1998); S. K. Turitsyn, E. G. Shapiro, S. B. Medvedev, M. P. Fedoruk., and V. K. Mezentsev, *Comp. Rend. Phys.* **4**, 145 (2003).
- [6] R. Grimshaw, J. He, and B. A. Malomed, *Phys. Scripta* **53**, 385 (1996).
- [7] A. Kaplan, B. V. Gisin, and B. A. Malomed, *J. Opt. Soc. Am. B* **19**, 522 (2002).
- [8] C. Paré, A. Villeneuve, P. A. Belanger, N. J. Doran, *Opt. Lett.* **21**, 459 (1996); C. Pare, A. Villeneuve, and S. LaRochelle, *Opt. Commun.* **160**, 130 (1999).

- [9] R. Driben, B. A. Malomed, M. Gutin, and U. Mahlab, Opt. Commun. **218**, 93 (2003); R. Driben, B. A. Malomed, and U. Mahlab, *ibid.* **232**, 129 (2004).
- [10] I. R. Gabitov and P. M. Lushnikov, Opt. Lett. **27**, 113 (2002); K. Beckwitt, F. O. Ilday, and F. W. Wise, *ibid.* **29**, 763 (2004); J. D. Ania-Castanon, I. O. Nasieva, N. Kurukitkoson, S. K. Turitsyn, C. Borsier, and E. Pincemin, Opt. Commun. **233**, 353 (2004).
- [11] F. O. Ilday and F. W. Wise, J. Opt. Soc. Am. B **19**, 470 (2002).
- [12] J. Atai and B. A. Malomed, Phys. Lett. A **298**, 140 (2002).
- [13] I. Towers and B. A. Malomed, J. Opt. Soc. Am. **19**, 537 (2002).
- [14] S. Carrasco, D. V. Petrov, J. P. Torres, L. Torner, H. Kim, G. Stegeman, and J. J. Zondy, Opt. Lett. **29**, 382 (2004).
- [15] R. Driben and B. A. Malomed, Opt. Commun. **185**, 439 (2000).
- [16] S. Inouye, M. R. Andrews, J. Stenger, H. J. Miesner, D. M. Stamper-Kurn, and W. Ketterle, Nature **392**, 151 (1998); J. L. Roberts, N. R. Claussen, J. P. Burke, C. H. Greene, E. A. Cornell, and C. E. Wieman, Phys. Rev. Lett. **81**, 5109 (1998); J. Stenger, S. Inouye, M. R. Andrews, H. J. Miesner, D. M. Stamper-Kurn, and W. Ketterle, *ibid.* **82**, 2422 (1999); S. L. Cornish, N. R. Claussen, J. L. Roberts, E. A. Cornell, and C. E. Wieman, *ibid.* **85**, 1795 (2000); E. A. Donley, N. R. Claussen, S. L. Cornish, J. L. Roberts, E. A. Cornell, and C. E. Wieman, Nature **412**, 295 (2001).
- [17] J. J. García-Ripoll, V. M. Pérez-García and P. Torres, Phys. Rev. Lett. **83**, 1715 (1999); J. J. García-Ripoll and V. M. Pérez-García, Phys. Rev. A **59**, 2220 (1999).
- [18] F. Kh. Abdullaev and R. Galimzyanov, J. Phys. B **36**, 1099 (2003).
- [19] H. Saito and M. Ueda, Phys. Rev. Lett. **90**, 040403 (2003); F. Kh. Abdullaev, J. G. Caputo, R. A. Kraenkel, and B. A. Malomed, Phys. Rev. A **67**, 013605 (2003); G. D. Montesinos, V. M. Pérez-García, and H. Michinel, Phys. Rev. Lett. **92**, 133901 (2004); G. D. Montesinos, V. M. Pérez-García, and P. J. Torres PJ, Physica D **191**, 193 (2004).
- [20] P. G. Kevrekidis, G. Theocharis, D. J. Frantzeskakis, and B. A. Malomed, Phys. Rev. Lett. **90**, 230401 (2003).
- [21] D. E. Pelinovsky, P. G. Kevrekidis, and D. J. Frantzeskakis, Phys. Rev. Lett. **91**, 240201 (2003).
- [22] D. Anderson, Phys. Rev. A **27**, 3135 (1983); B. A. Malomed, Progr. Opt. **43**, 71 (2002).
- [23] J. Satsuma, and N. Yajima, Progr. Theor. Phys. (Suppl.) **55**, 284 (1974).